SCIENCE CHINA
Earth Sciences

• RESEARCH PAPER •

December 2015 Vol.58 No.12: 2309–2326
doi: 10.1007/s11430-015-5197-0

Modeling permafrost properties in the Qinghai-Xizang (Tibet) Plateau

HU GuoJie, ZHAO Lin*, WU XiaoDong, LI Ren, WU TongHua, XIE ChangWei, PANG QiangQiang, XIAO Yao, LI WangPing, QIAO YongPing & SHI JianZong

Cryosphere Research Station on Qinghai-Xizang Plateau, State Key Laboratory of Cryospheric Sciences, Cold and Arid Regions Environmental and Engineering Research Institute, Chinese Academy of Sciences, Lanzhou 730000, China

Received February 11, 2015; accepted June 3, 2015; published online September 24, 2015

Water and heat dynamics in the active layer at a monitoring site in the Tanggula Mountains, located in the permafrost region of the Qinghai-Xizang (Tibet) Plateau (QXP), were studied using the physical-process-based COUPMODEL model, including the interaction between soil temperature and moisture under freeze-thaw cycles. Meteorological, ground temperature and moisture data from different depths within the active layer were used to calibrate and validate the model. The results indicate that the calibrated model satisfactorily simulates the soil temperatures from the top to the bottom of the soil layers as well as the moisture content of the active layer in permafrost regions. The simulated soil heat flux at depths of 0 to 20 cm was consistent with the monitoring data, and the simulations of the radiation balance components were reasonable. Energy consumed for phase change was estimated from the simulated ice content during the freeze/thaw processes from 2007 to 2008. Using this model, the active layer thickness and the energy consumed for phase change were predicted for future climate warming scenarios. The model predicts an increase of the active layer thickness from the current 330 cm to approximately 350–390 cm as a result of a 1–2°C warming. However, the effect active layer thickness of more precipitation is limited when the precipitation is increased by 20%–50%. The COUPMODEL provides a useful tool for predicting and understanding the fate of permafrost in the QXP under a warming climate.

permafrost, COUPMODEL, hydrothermal processes, phase change, soil temperature, soil moisture

Citation: Hu G J, Zhao L, Wu X D, Li R, Wu T H, Xie C W, Pang Q Q, Xiao Y, Li W P, Qiao Y P, Shi J Z. 2015. Modeling permafrost properties in the Qinghai-Xizang (Tibet) Plateau. Science China: Earth Sciences, 58: 2309–2326, doi: 10.1007/s11430-015-5197-0

Permafrost, which is defined as ground in which temperatures have remained at or below 0°C for at least two consecutive years, is a key component of the cryosphere due to its influence on energy exchanges, hydrological processes, natural hazards, and carbon budgets and hence the global climate system (Riseborough et al., 2008). Permafrost has been treated as an indicator of climate change and is highly sensitive to climate changes (Pavlov, 1994; Guglielmin and Dramis, 1999; Smith et al., 2002). Climate warming has a significant influence on permafrost, which has caused extensive degradation all over the world (Lunardini, 1996; Stendel and Christensen, 2002; Zhang, 2005; Wang et al., 2005; Cheng and Wu, 2007; Wu et al., 2010; Wei et al., 2011). Permafrost responds quickly to climate change, and this rapid response leads to dramatic changes in the soil physical and chemical properties, water and heat dynamics, and nitrogen and carbon cycles (Hansson et al., 2004; IPCC, 2007). Previous research predicted that thawing of permafrost might cause serious societal and environmental problems in the 21st century (Brown et al., 2008). Therefore, increasing attention has been focused on understanding, assessing, and predicting the changes in the permafrost under climate change scenarios.

*Corresponding author (email: linzhao@lzb.ac.cn)

Permafrost changes will provide feedback on the climate system through the active layer (Kane et al., 1991; Poutou et al., 2004). Defined as the portion that thaws in summer and freezes in winter, the active layer is an important component of permafrost and the resultant exchange of water and heat. Thus, the changes in the active layer have a great influence on ecological systems, surface energy balances, engineering construction, and hydrological and carbon cycles in permafrost regions (Kane et al., 1991; Zhang et al., 2005; Wang et al., 2014). Permafrost changes occur via the hydrothermal characteristics of the active layer, and hydrothermal change can lead to water-heat exchange differences and large-range alterations in the sensible and latent heat (Ma et al., 1999). These changes can cause further alterations in atmospheric circulation and thus impact the climate system (Vinnikov et al., 1996; Allisonet al., 2001). The importance of soil hydrothermal processes has been recognized over the last several years (Hansson et al., 2004), but less attention has been given to the effect of climate conditions on the freezing and thawing processes in the soil. This knowledge is important for improving human capacity to act on global climate change in future and could improve our understanding of the interaction between soil freeze-thaw processes and climate change.

Process-based modeling is an important approach for studying the interactions among the atmosphere, vegetation, and hydro-thermal processes (Sridhar et al., 2002). During the past decades, a number of different numerical models have been developed to study frozen soil water-heat processes, i.e., the Harlan (Harlan, 1973), FROSTB (Shoop and Bigl, 1997), SHAW (Nassar et al., 2000; Zhao et al., 2008), and CLM3 models (Alexeeve et al., 2007; Nicolsky et al., 2007). Certain models were also proposed to study permafrost thermal conditions (Ikard et al., 2009; Oelke and Zhang, 2004), permafrost and climate change, and permafrost distribution, i.e., TTOP (Henry and Smith, 2001; Riseborough, 2002; Luo et al., 2014), as well as models for analyzing the relationship between permafrost and climate change (Buteau et al., 2004; Jiang et al., 2012; Hollesen et al., 2011). Recently, the soil-vegetation-atmosphere system (SVAT) model has been widely applied to soil for modeling of hydrothermal processes process, i.e., the COUPMODEL (Scherler et al., 2010; Wu et al., 2011a, 2011b, 2012; Zhou et al., 2013; Zhang et al., 2007; Yang et al., 2010; Hu et al., 2013). The COUPMODEL considers the influence of ice on soil moisture migration (Jansson and Karlberg, 2004). Predictions of ice are notable outputs from COUPMODEL that improve our knowledge of the course of ice during freeze-thaw periods (Wu et al., 2011a). With this model, research studies have been able to achieve good results for the permafrost of the Heihe Mountains (Yang et al., 2010) and the Qinghai-Xizang Plateau (QXP) region (Zhou et al., 2013; Zhang et al., 2007; Hu et al., 2013) in China. These results have improved our understanding of the hydro-thermal processes in the permafrost regions. However, the simulated depth was shallow, and previous work lacked an analysis of surface heat change. Therefore, this topic requires further study of the water-thermal characteristics of the permafrost active layer.

Approximately 1.4×10^6 km^2 of permafrost exists in the Qinghai-Xizang (Tibet) Plateau (QXP) (Cheng and Zhao, 2000). The QXP is one of the areas that is most sensitive to global climate change and is a climate change initiation area for China (Liu and Chen, 2000; Tang et al., 1979). Many land surface process models have been used to study the frozen soil water-heat processes in the permafrost regions of the QXP (Wu et al., 2003; Zhang et al., 2003; Gao et al., 2004; Wang and Shi, 2007; Luo et al., 2008). So far, the existing land surface process models are considered more appropriate for the uniform underlying surface conditions and have ignored permafrost or have been used only for rather simple generalization (Hu et al., 2006). Additionally, a detailed awareness of the land surface is needed for the permafrost regions of the Qinghai- Xizang (Tibet) Plateau of China (Wang and Shi, 2007). In such a low latitude alpine region, the characteristics of solar radiation, air temperature, wind speed, and snow cover are very different from those at high latitudes (Xiao et al., 2013). In addition, the permafrost of the plateau is much thinner and is more sensitive to changes in climate changes and surface conditions (Cheng, 1990). Therefore, it is of great importance to study the hydro-thermal processes in this area. In this study, the COUPMODEL was used to simulate the hydro-thermal processes, analyze the heat balance characteristics, and estimate the ice content and the energy consumed for phase change in the QXP. The objectives of the current study were to: (1) evaluate the performance of the COUPMODEL simulation in the QXP, (2) estimate the ice content and calculate the energy consumed for phase change, and (3) predict and demonstrate the effect of increasing air temperature and precipitation on the active layer thickness in the Tanggula test site in the Qinghai-Tibet Plateau of China.

1 Study areas

1.1 Study site

With an altitude of 5100 m, the studied Tanggula site (33°04′N and 91°56′E) is situated on a gentle slope at the Tanggula Mountains in the Qinghai-Tibet Plateau of China. The monitoring site (Figure 1) is located in the continuous permafrost zone, and the underlying surface belongs to an alpine meadow (Yao et al., 2008). The vegetation consists of alpine meadow distributed in clusters with heights of less than 10 cm and coverage of approximately 20% to 30%.The observation site was established in June 2004.

1.2 Data

1.2.1 Monitoring data

The hourly meteorological data, consisting of precipitation,

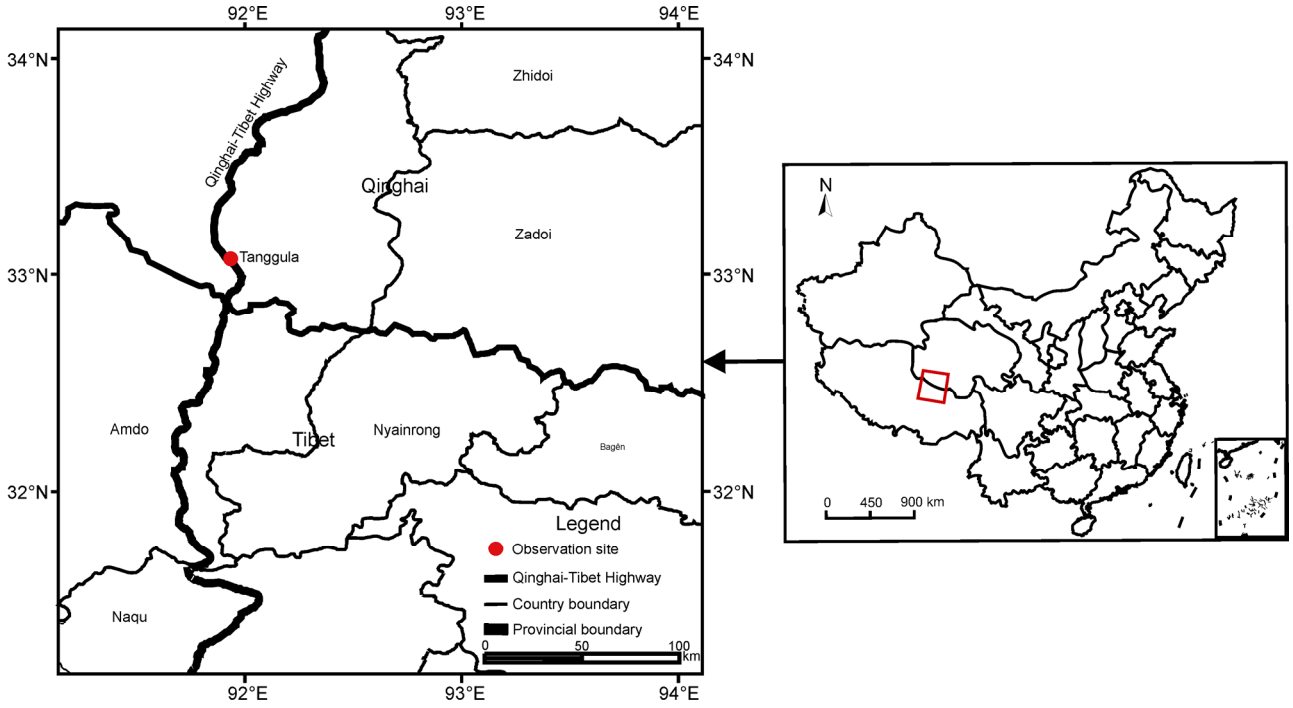

Figure 1 Location of the Tanggula comprehensive observation site on the Qinghai-Xizang (Tibet) Plateau in China.

global radiation, net radiation, air temperature, wind speed and relative humidity measurements, were recorded using a CR23X data acquisition instrument (Campbell Scientific Inc.). The air temperature, relative humidity, and wind speed were measured at heights of 2 and 10 m. The snow depth was measured by SR50 snow depth instrument (Campbell, USA). The soil temperature and moisture in the active layer were recorded every 0.5 h by a CR1000 data acquisition instrument (Campbell Scientific Inc.) at different depths (Xiao et al., 2013). The data used in this study are the daily mean values.

1.2.2 Atmospheric forcing data

This study was carried out from 1 January 2007 to 31 December 2008. The meteorological variables used as the driving variables in the simulations presented here were daily air temperature, relative air humidity, wind speed, precipitation, global radiation and surface soil temperature. Atmospheric forcing data include atmospheric temperature (°C), wind speed (m/s), relative humidity (%), precipitation (mm), new snow (cm), and global solar radiation (W/m^2), all observed at the Tanggula site. The mean annual air temperature was −4.4 and −5.8°C and the annual precipitation was 544 and 488 mm in 2007 and 2008. Precipitation is normally concentrated in the period from May to September. The minimum air temperature was −20.3 and −25.2°C, and the maximum was 8.5 and 7.5°C in 2007 and 2008. The active soil layer thickness is about 3 m in the site.

1.2.3 Surface parameters

In the model, some parameters have a default value, but many parameters, such as latitude, slope, surface roughness, TempAirAmpl, TempAirMean, Albedo, TempDiffPrec_Air, initial temperatures, initial water content, surface temperature, heat flux, etc., were calibrated by measurements (Table 1).The samples were analyzed in the laboratory to determine the soil bulk density and soil texture with respect to sand, silt, and clay (Table 2).

(1) Surface temperature calculations. For soil depths from 0 to 5 cm, the soil temperature was measured at 2 and 5 cm at the Tanggula test site. The thickness of the soil is relatively small from the surface to a 5 cm depth, and the soil texture is uniform. Soil temperature changes can be considered as linear, and the gradient is the same throughout the area. In this case, surface temperature is estimated as described previously (Zhao et al., 2008) as

$$\Delta T_1/\Delta Z_1=\Delta T_2/\Delta Z_2, \tag{1}$$

$$T_0=(5T_{s2}-2T_{s5})/3, \tag{2}$$

where $\Delta T_1=T_{s2}-T_0$, $\Delta Z_1=0.02$, $\Delta T_2=T_{s5}-T_{s2}$, $\Delta Z_2=0.03$, T_0 is the surface temperature, and T_{s2} and T_{s5} are soil temperatures at 2 and 5 cm depths, respectively.

(2) Surface heat flux calculations. The surface heat flux G_0 is calculated according to

$$G_0 = G_z + C_s\int_0^z \frac{\partial T}{\partial t}\mathrm{d}z \approx G_z + C_s\frac{\Delta T}{\Delta t}z, \tag{3}$$

where z is the soil depth at 5 cm, G_z is the soil heat flux observed at 5 cm depth, T is the soil temperature at 5 cm depth, and C_s is the volumetric soil heat capacity (J/(m^3 K)).

Table 1 Parameters adjusted in the simulations

Parameter	Value	Source
Latitude	33.07°N	Measurements
Slope	0°	Measurements
Albedo (dry soil)	0.25	Zhang et al. (2007); Xiao (2013)
Altsimstation	5100 m	Measurements
TempAirAmpl	32°C	Calculated
TempAirMean	–4.7°C	Calculated
TempDiffPrec_Air	–3°C	Calibrated
FreezepointF1	30.5	Calibrated
FreezepointFWi	0.8	Calibrated
HighFlowDampC	46.1%	Calibrated
LowFlowCondImped	5.8	Calibrated
Initial temperatures:eg.layer1	–10.6°C	Measurements
Initial water content:eg.layer1	10%	Measurements

In the northern Xizang Plateau, C_s is taken as 1.18×10^6 (J/(m^3 K))(Xiao et al., 2011) which is the annual average value in this area.

2 Methods

2.1 Model description

The COUPMODEL is a one-dimensional SVAT model that simulates fluxes of water, heat, carbon, and nitrogen in the soil-plant-atmosphere system (Jansson and Moon, 2001; Jansson and Karlberg, 2004) by coupling the former SOIL (McGechan et al., 1997) and SOILN (Eckersten et al., 2001) models. The COUPMODEL is a fairly complex model that simulates water and heat processes in the soil based on well-known physical equations. Two coupled differential equations for water and heat flow based on quality and energy conservation represent the core of the model.

In cold regions in China, when the soil temperature is above 0°C or below T_f (the soil completely frozen when the temperature is below T_f), the soil is either non-frozen or completely frozen. In this case, there is no water-ice/ice-water conversion process. The simple Darcy's law and the heat conduction equation can be solved using soil water and heat movement. However, when the soil temperature is between 0°C and T_f, the soil water movement and heat conditions are closely linked and highly complex, and the soil pore size distribution, thermal conductivity, and hydraulic conductivity will change with the changes of the soil water content. Thus, the model must take into account the soil water heat coupling process, which is the essence of COUPMODEL (Yang et al., 2010). Under partially frozen conditions the soil can be considered to consist of two flow domains, one consisting of small pores where water is unfrozen due to a low water potential, and another consisting of large pores that are air-filled because of surface tension effects. In the former one consisting of small sized pores the flow will consequently be much slower than in the high-flow domain, and this domain is thus called the low-flow domain. An important advantage of the model is the limited input data required to obtain more reasonable and satisfactory simulation results (Jansson and Karlberg, 2004). In this paper, we give a brief description of the important heat and moisture modules of the model that were used in our simulations.

(1) Soil Heat Process. Soil heat flow in the soil is expressed as the sum of conduction, water, and vapor convection:

$$q_h = -k_h \frac{\partial T}{\partial z} + C_w T q_w + L_v q_v, \tag{4}$$

where q_h is the heat fluxes (J/(m^2 day)), q_w and q_v are water, and vapor (mm/day), respectively, k_h is the thermal conductivity (J/(m s °C)), T is the soil temperature (°C), C_w is the soil water heat capacity (J/(m^3 °C)), L_v is the latent heat of vaporization (J/kg), and z is the depth (m).

The upper boundary condition is determined by eq. (5):

$$q_h(0) = -k_{ho} \frac{(T_S - T_1)}{\Delta z/2} + C_w (T_a - \Delta T_{pa}) + L_v q_{vo}, \tag{5}$$

where k_{ho} is the conductivity of organic material at surface (J/(m^3 s °C)), T_S is the surface temperature (°C), T_1 is the temperature in the uppermost soil layer (°C), ΔT_{pa} is a parameter that represents the temperature different between the air and the precipitation (°C), q_{in} is the water infiltration

Table 2 Soil texture parameters used as inputs for COUPMODEL

Soil depth (cm)	Sand (%)	Silt (%)	Clay (%)	Soil depth (cm)	Sand (%)	Silt (%)	Clay (%)
0–2	85	10	5	49–83	85	10	5
2–5	85	10	5	83–138	95	3	2
5–9	75	18	7	138–230	90	5	5
9–17	70	18	12	230–380	68	20	12
17–29	65	22	13	380–628	95	3	2
29–49	85	10	5	–	–	–	–

rate(m/s), q_{vo} is the water vapor flow (m/s) and L_v is the latent heat (W/m^2).

The lower boundary condition is determined by eq. (6):

$$T_{LowB} = T_{amean} - T_{aamp} \mathrm{e}^{-\frac{z}{d_a}} \cos((t - t_{ph})\omega - z/d_a), \quad (6)$$

where t is the time, t_{ph} is the phase shift, ω is the frequency of the cycle and z is the soil depth, d_a is the damping depth and annual mean air temperature, T_{amean}, and amplitude, T_{aamp}, are the parameters.

(2) Soil Water Flow. Soil water flow is assumed to obey Darcy's law as generalized for unsaturated flow by Richards

$$q_w = -k_w \left(\frac{\partial \psi}{\partial z} - 1 \right) - D_v \frac{\partial c_v}{\partial z}, \quad (7)$$

where k_w is the unsaturated hydraulic conductivity (m/s), ψ is the water tension (m), z is the depth (m), c_v is the concentration of vapour flow and D_v is the diffusivity coefficient (m^2/s) for vapour in the soil.

(3) Surface Energy Balance Approach. According to the law of conservation of energy, net radiation at soil surface is equal to the sum of latent flux, sensible heat flux and heat flux to the soil:

$$R_{ns} = L_v E_S + H_S + q_h, \quad (8)$$

where L_vE_S is the sum of latent heat flux (W/m^2), H_S is sensible heat flux (W/m^2) and q_h is heat flux to the soil (W/m^2).

Latent heat flux is calculated according to:

$$L_v E_S = \frac{\rho_a c_p}{\gamma} \frac{\left(e_{surf} - e_a\right)}{r_{as}}, \quad (9)$$

where r_{as} is the aerodynamic resistance (s/m), e_{surf} is the vapour pressure at the soil surface (Pa), e_a is the actual vapour pressure in the air (Pa), ρ_α is the air density (kg/m^3), c_p is the heat capacity of air (J/(kg °C)), L_v is the latent heat of vaporization (W/m^2) and γ is the psychometric constant (kg/m^3).

Sensible heat flux is calculated according to:

$$H_S = \rho_a c_p \frac{\left(T_s - T_a\right)}{r_{as}}, \quad (10)$$

where T_s is the soil surface temperature (°C), T_a is the air temperature (°C) and r_{as}, ρ_a, c_p are the same as above.

2.2 Model application

The model input data include atmospheric forcing data and the basic information and surface parameters of the study region. The zero depth annual amplitude with a constant geothermal flux is measured at a mean depth of approximately 15 m over the hinterland of the QXP. To obtain a better simulation of changes in the permafrost, we increased the number of soil layers to 30, extending the lower boundary to a depth of 17 m. The simulated soil profile (0–17 m) was composed of 30 soil layers, i.e., 17 soil layers from 0 to 400 cm and 13 soil layers located at every meter from 4 to 17 m. The simulated soil profile (0–17 m) was composed of 30 soil layers, i.e., 17 soil layers (0, 2, 5, 10, 20, 35, 50, 70, 90, 105, 140, 175, 210, 245, 280, 300, 350, and 400 cm) and 13 soil layers located at every meter from 4 to 17 m.

The root mean square error (RMSE) was used to evaluate the simulation results. The R^2, the determination coefficient of the linear regression between the simulated and measured values, and ME, the mean error of the model, were used in this study.

2.3 Latent heat consumed for phase change calculations

Based on the simulated ice content results for the process of freezing and thawing, latent heat consumed for phase change was calculated at depth 0–400 cm according to

$$Q = \sum_{i=1}^{31} M_i \times 335/1000, \quad (11)$$

where Q is the total monthly phase heat, the ice latent heat is 335 kJ/kg, and M_i is the daily phase heat determined by eq. (14):

$$M_i = \left(\frac{\sum_{n=1}^{17} V_n}{100} \times Z_n \right) \times \rho_{\mathrm{ice}}, \quad (12)$$

where V_n is the n-layer simulated volume of ice (%); Z_n is the n-layer thickness (m),and ρ_{ice} is 917 kg/m^3. In order to include all energy consumed for phase change of the active layer, we considered the 400 cm depth for calculating.

Compared with another method, the water-ice phase change heat was also calculated using the measured temperature and unfrozen water content with the following three assumptions (Zhao, 2004):

(1) The water begins to freeze at a temperature of 0°C, and the latent heat is 333.6 J/g.

(2) After the ground surface and the active layer was completely frozen, the water migration from the surface ground to the active layers and the migration from the bottom of the active layer to permafrost is ignored since the unfrozen water under this circumstance was low and the vertical migration rates were very low (Tian et al., 2014).

(3) The frozen water all melts during the melt season, i.e., the freezing phase change heat was equal to the melting phase change heat.

2.4 Selection of future scenarios

Soil temperatures at shallow depths are sensitive to air tem-

perature, and ALT is highly responsive to warming air temperatures (Hinkel and Nelson, 2003; Demchenko et al., 2006). The air temperature increased by 0.25°C/10 a from 1961 to 2002 in the QXP (Wang et al., 2005). Wu et al. (2008) showed that mean annual permafrost temperatures at 6.0 m depth have increased by 0.12 to 0.67°C with an average increase of approximately 0.43°C during the past decade using data from 10 boreholes along the Qinghai-Xizang an Highway from 1996 through 2006. Additionally, using the outputs as simulated by 13 GCM models provided by the IPCC (2007), the situation results predicted that air temperatures will rise and annual precipitation will increase under different scenarios (A2, A1B, and B1) in China (Jiang et al., 2008). The result of an 11-model ensemble mean shows that the air temperature and precipitation will increase by 1.98°C and 0.06 mm/d (which accounted for 45% of the measured annual precipitation in 2008) in the mid-21st century compared with data in 2008 under the A1Bscenarios, and significant wetting and warming trends will occur over the Qinghai-Xizang (Tibet) Plateau in the next 100 years (Cheng et al., 2011). Therefore, an investigation into the influence of climatic warming on the active layer was conducted by comparing the modeled soil temperature profiles under five scenarios (air temperature increasing by 1 and 2°C with no precipitation and 20% and 50% additional precipitation) for a changing annual mean air temperature and precipitation.

3 Results

3.1 Simulation of the soil temperature

The model predicted the soil temperature for all treatments reasonably well during the course of the 2-year experiment from January 2007 to December 2008. The residuals were calculated using the measured minus modeled values (Figure 2). The model results appear to show higher temperatures for deeper soil profiles during March to September for both years. In spring, the snowmelt water infiltrates into the near-surface soil horizons and subsequently re-freezes, thus creating a period during which temperatures hover at approximately 0°C. In fall, temperatures persist at 0°C due to the effects of latent heat exchange during phase change, commonly referred to as the "zero-degree curtain" (zero-degree contours). Based on our simulations, these zero-degree temperatures at the seasonal boundaries (spring thaw and fall freeze-up) could persist for several days or weeks in the spring and fall. Figure 3 illustrates the comparison of the two-layer soil temperatures at deeper layers with depths of 5 m and 10 m. The comparison shows that the simulated soil temperatures closely match the observations.

The modeled soil temperatures are comparable with the observations throughout the entire soil profile (Table 3). However, the discrepancy between the modeled and measured soil temperatures increases with profile depth. For example, the root mean square error (RMSE) from a comparison between the modeled and measured soil temperatures generally increases from the top to bottom soil layers. The regression coefficient R^2 was notably close to 1, and the RMSE was less than 1°C from 0 to 105 cm, which revealed that the simulated results agreed well with the measured values. In the 175–300 cm layer, the simulation accuracy decreased, but the R^2 was greater than 0.94, the RMSE was less than 1°C, and the ME was less than 0.5°C. Overall, the average R^2, RMSE, and ME values were 0.97, 0.74, and 0.13°C, respectively. These results indicated that the simulated

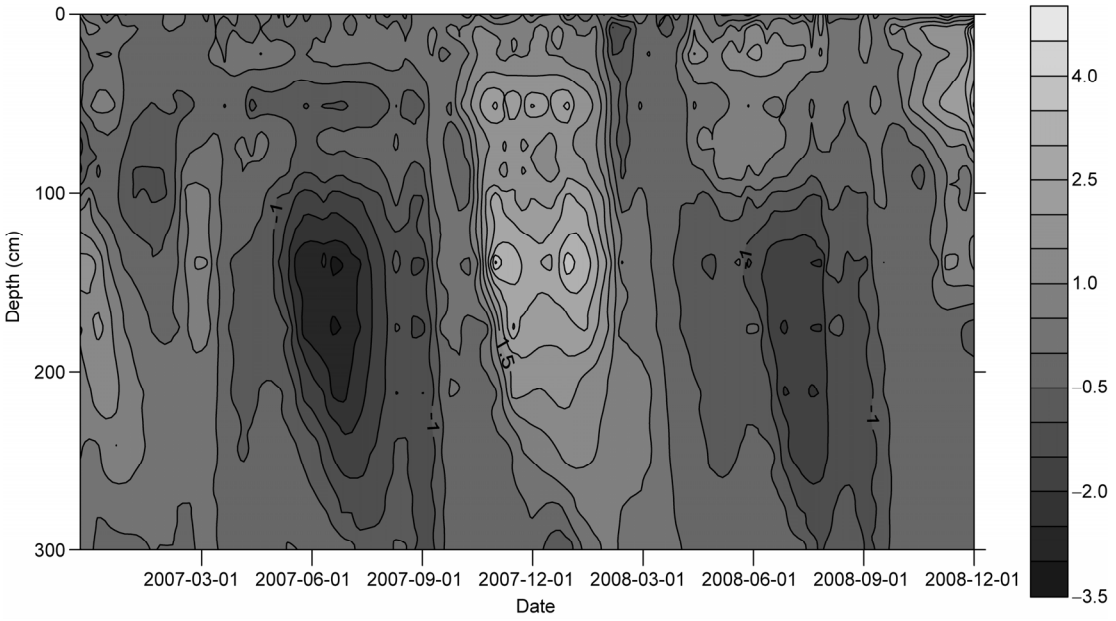

Figure 2 Soil temperature residuals (°C) between modeled and measured soil temperatures.

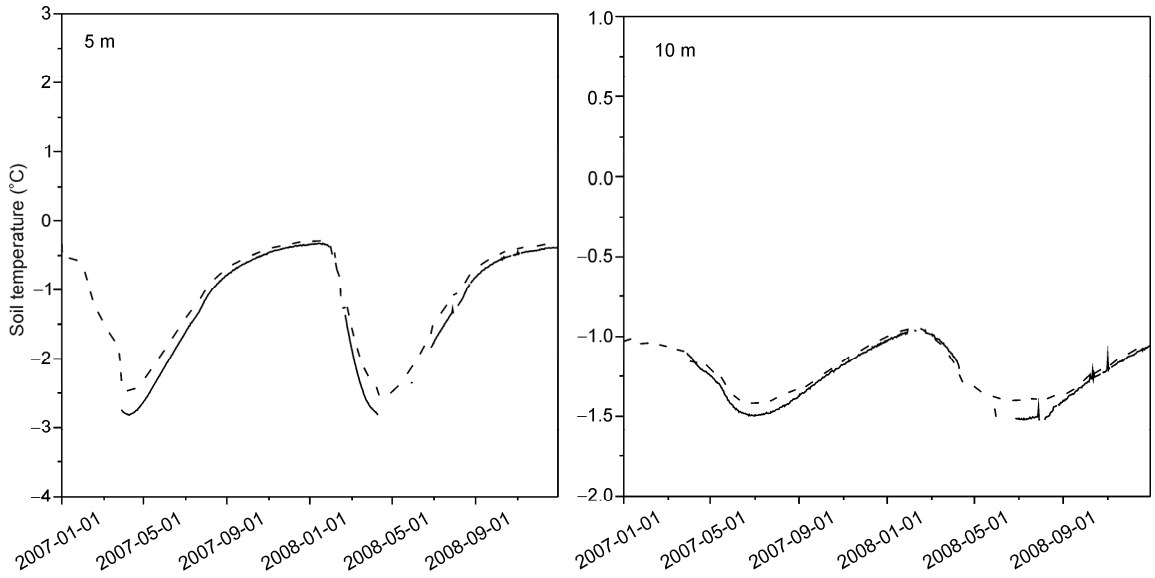

Figure 3 Modeled (dashed line) and measured (solid line) soil temperatures from a borehole at 5 and 10 m.

Table 3 Comparative analysis of the simulated and observed soil temperatures at different depths

Soil depth (cm)	R^2	ME (°C)	RMSE (°C)	Soil depth (cm)	R^2	ME (°C)	RMSE (°C)
2	0.99	–0.22	0.74	105	0.98	0.31	1.1
5	0.99	–0.22	0.7	140	0.97	0.34	1.24
10	0.99	–0.27	0.66	175	0.95	0.4	0.89
20	0.99	–0.32	0.7	210	0.93	0.42	0.85
50	0.99	–0.08	0.62	245	0.93	0.4	0.64
70	0.99	0.06	0.71	280	0.92	0.41	0.65
90	0.99	0.22	0.58	300	0.89	0.44	0.74

soil temperature results of the model are more desirable. The R^2 was greater than 0.9 at depths of 5 and 10 m, which indicates that the calibrated model results in a better simulation of soil temperature at the deep layers with smaller error.

3.2 Simulation of the soil moisture

The model predicted the soil moisture (all unfrozen water content) well during the course of the 2−year experiment. The results show that the simulated values were consistent with the monitored values at a depth of 5–20 cm but were less than the observed value in the freeze period. As the depth increases, the results simulated at a depth of 35–210 cm were better than those at the surface (Figure 4). In the 245–300 cm layer, the measured soil water content increased significantly and reflected that the deep soil moisture conditions were better because the soil moisture gathered in the freezing front.

The R^2 between the simulated and measured values ranged from 0.64 to 0.92. The RMSE values were less than 6.00 except for depths of 280 and 300 cm, where they were 7.42 and 9.54, respectively (Table 4). The ME were also large in the deepest locations of 280 and 300 cm, where they were −6.39 and −7.85, respectively. In most cases, the model predicted higher water contents than the measured values. The simulated soil moisture in the 5–210 cm layer showed good agreement with the measured values, but the accuracy relatively decreased in the 245–300 cm layer. Overall, the average R^2, RMSE, and ME values were 0.82, 5.15, and –0.64, respectively, which indicated that the error between the model simulation and observations of soil moisture was acceptable, and the results generally reflect the actual situation.

3.3 Surface heat balance

The soil heat flux reflects the thermal characteristic of the soil, and the surface heat flux (0 cm) was calculated according to eq. (3). The heat flux at a depth of 0–20 cm soil was simulated by the model, and the simulated values had large amplitudes (Figure 5). In the 0–20 cm layer, the R^2 values were 0.77, 0.82, 0.89 and 0.92, and the RMSEs were 7.97, 5.42, 4.28 and 3.6 W/m^2, respectively.

The net radiation (R_n) during the 2-year study period was

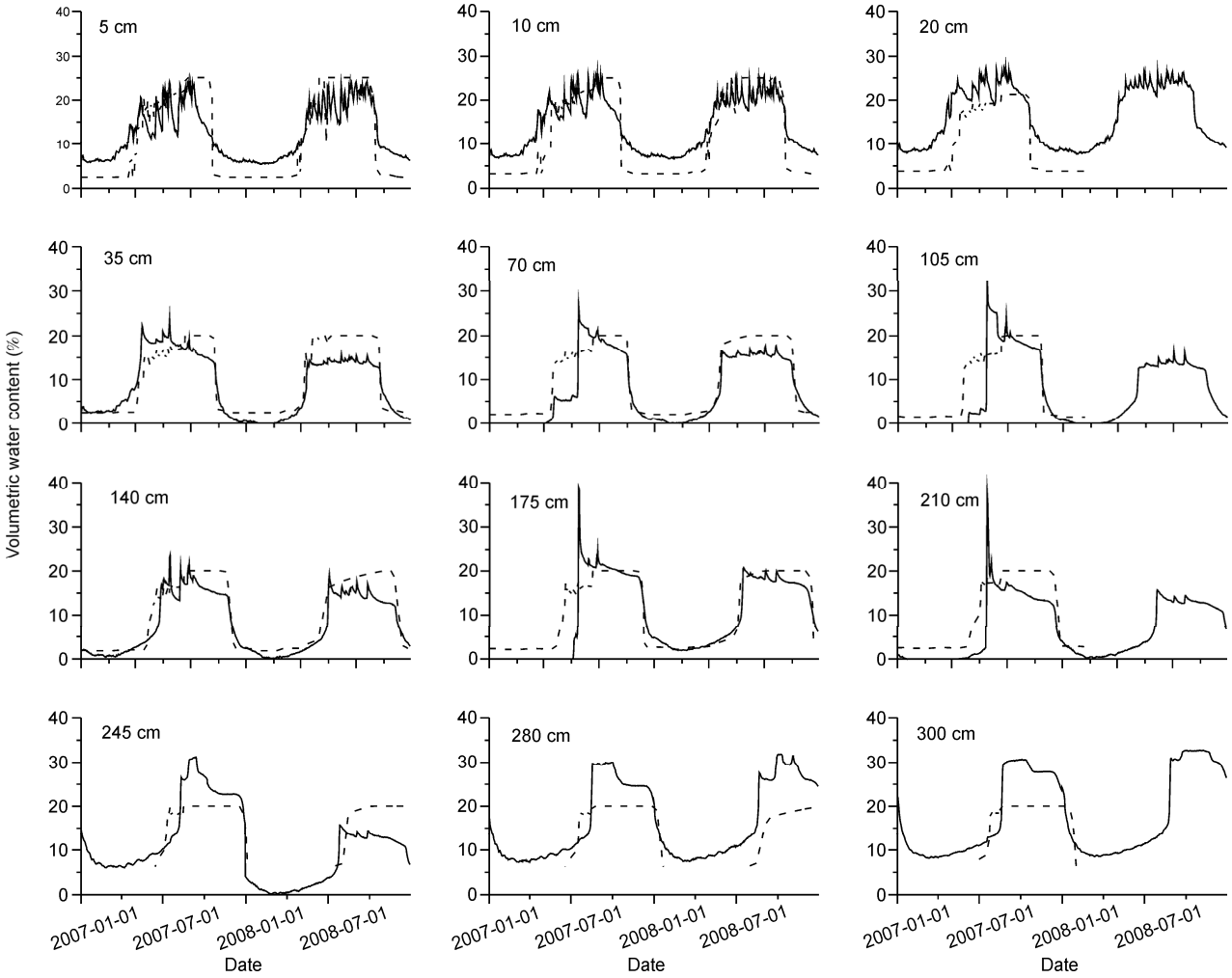

Figure 4 Modeled (dashed line) and measured (solid line) soil moisture at different depth.

Table 4 Comparative analysis of the simulated and observed soil moisture at different depths

Soil depth (cm)	R^2	ME	RMSE	Soil depth (cm)	R^2	ME	RMSE
5	0.81	–0.73	5.31	140	0.92	2.09	3.28
10	0.87	–1.69	4.92	175	0.83	1.19	3.84
20	0.9	–4.83	5.54	210	0.88	3.49	4.44
35	0.82	1.55	3.76	245	0.64	0.28	5.05

less than the measured values, most likely because of errors in the initial snow depth. Additionally, the net radiation was greater than the measured values from November 2008. However, the results closely followed the pattern of observed net radiation (Figure 6(a)). The partitioning fluxes of net radiation (LE, H, and G) during the two years varied considerably. The R^2 values for R_n, H, LE, and G were 0.79, 0.65, 0.83, and 0.77, respectively (Figure 6(a)–(d)). First, the monthly latent heat flux (LE) showed a seasonal pattern following the variation in monthly R_n, and the minimum values were reached during December and March. The average of the annual LE decreased from 47.6 to 39.8 W/m^2 (Figure 7). Second, the average of the annual H decreased substantially from 31.7 to 26.6 W/m^2 during 2007–2008, implying increasing temperature gradients between the air and the soil surface from year to year. Third, the averages of the annual G was 0.86 and 0.51 W/m^2 in 2007 and 2008, approximately 0 W/m^2.

3.4 Estimation of ice contents and energy consumed for phase change

The simulated ice contents at 50 cm were used as an example to demonstrate the ice conditions in the permafrost (Figure 8).

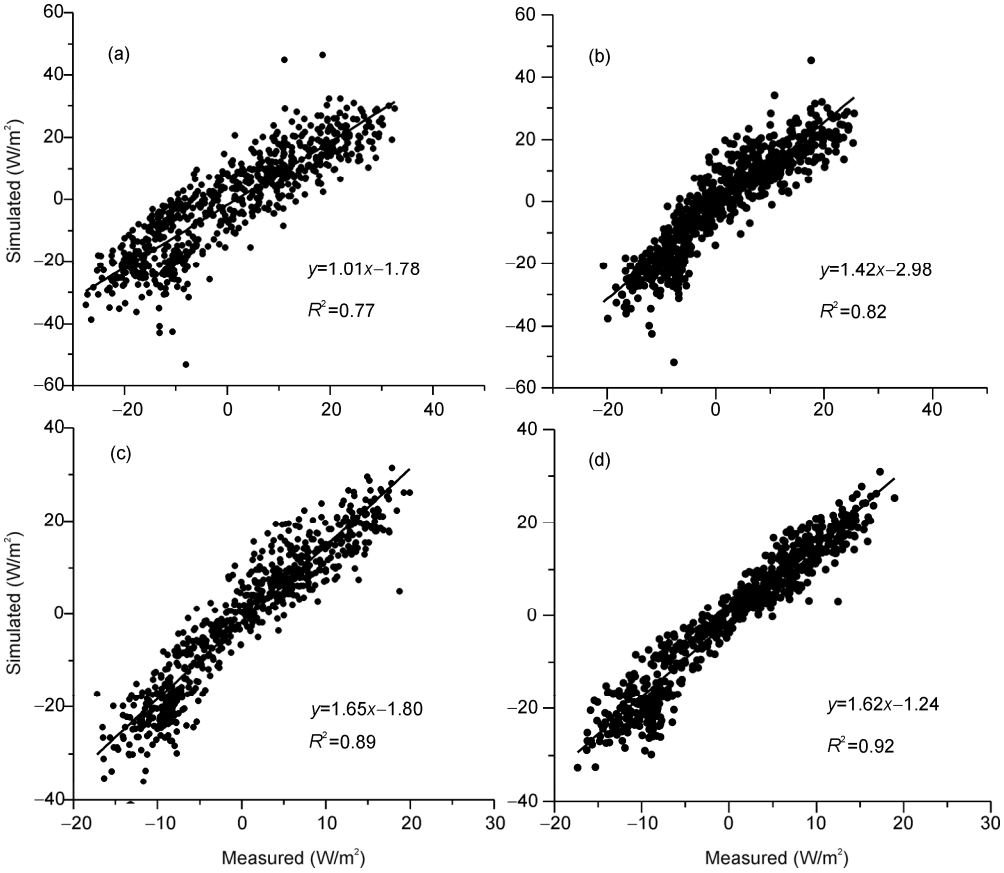

Figure 5 Modeled soil heat flux: 0 cm (a), 5 cm (b), 10 cm (c), and 20 cm (d).

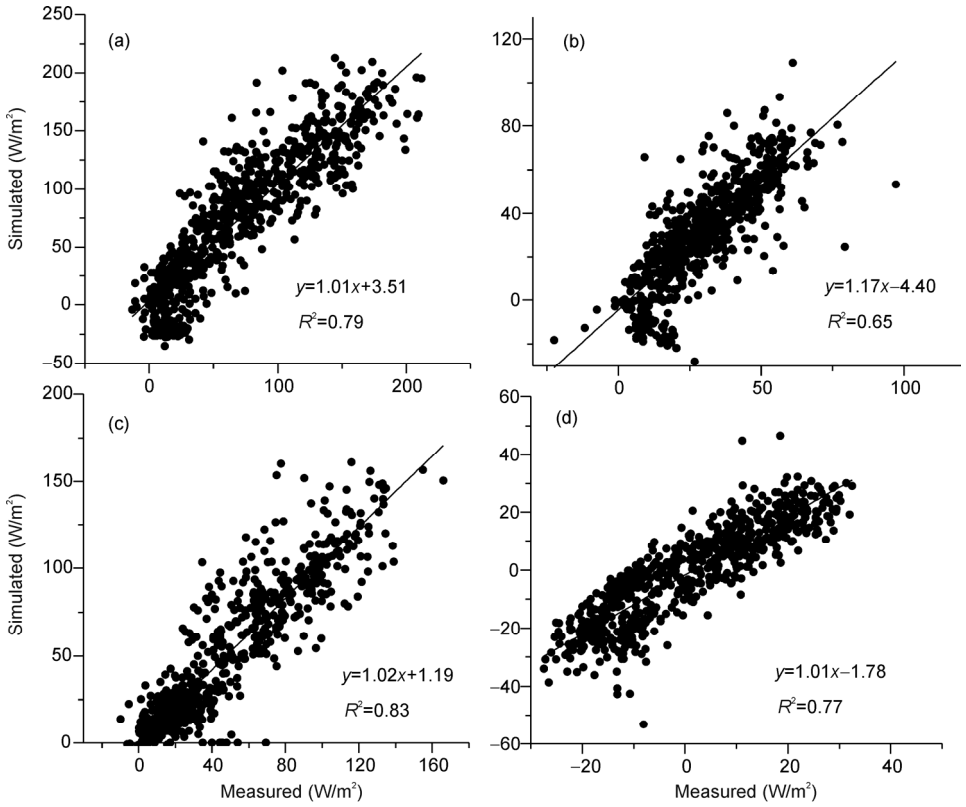

Figure 6 Calculated and observed: (a), net radiation heat flux; simulated and observed: (b) sensible heat flux, (c) latent heat flux and (d) soil surface heat flux.

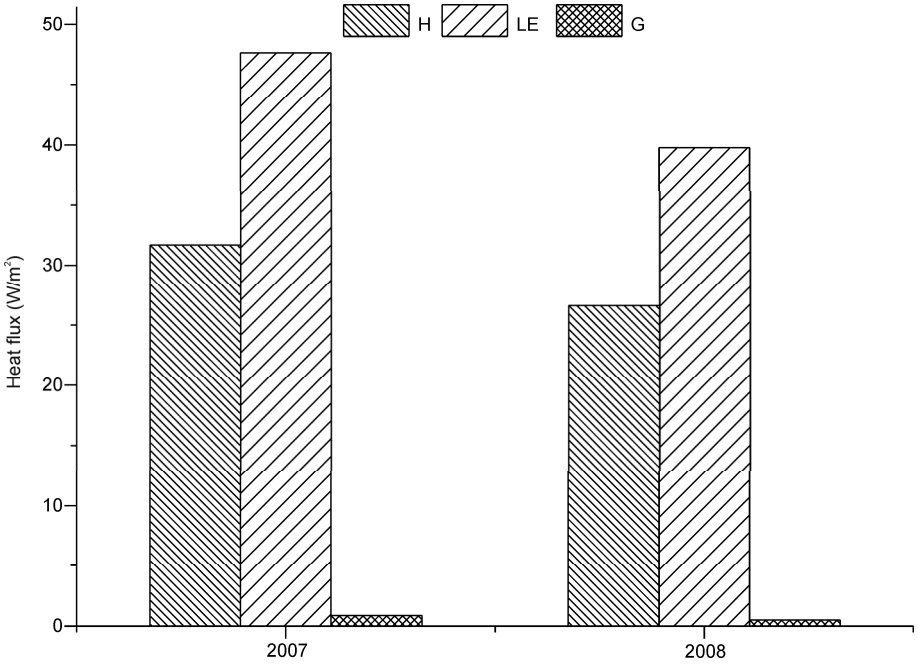

Figure 7 Average annual variations of sensible heat flux, latent heat flux and soil surface heat flux.

The soil ice content at 50 cm appeared from January and disappeared at the end of December during the two years (shown as the grey area in Figure 9). The ice content in the soil at 50 cm varied in a stable manner within the range of 2%–25%. The total water content (ice+liquid water) during the freeze-thaw periods was much larger than the liquid water content in the final days before the thaw periods began. The rapid and large changes in the volumetric water content indicate that use of only the measured total water content to predict ice content may result in a large uncertainty in the difference between the total water content and the estimated unfrozen water content.

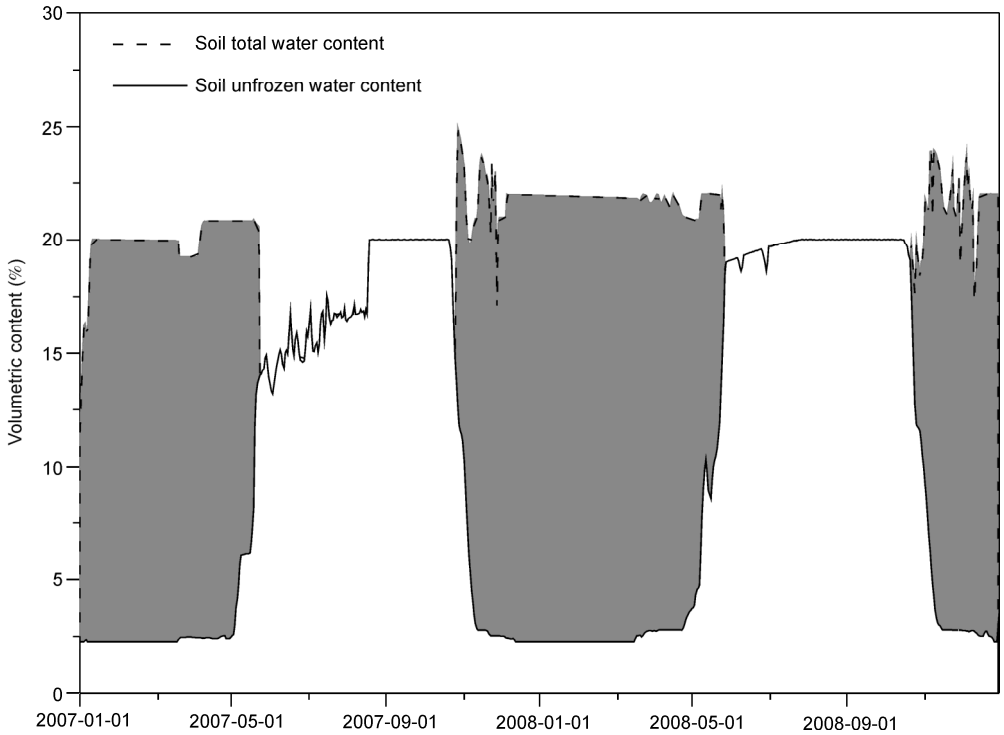

Figure 8 Modeled soil liquid water content (solid line) and soil total water content (dashed line) at 50 cm during 2007–2008. The grey area represents the estimated soil ice content.

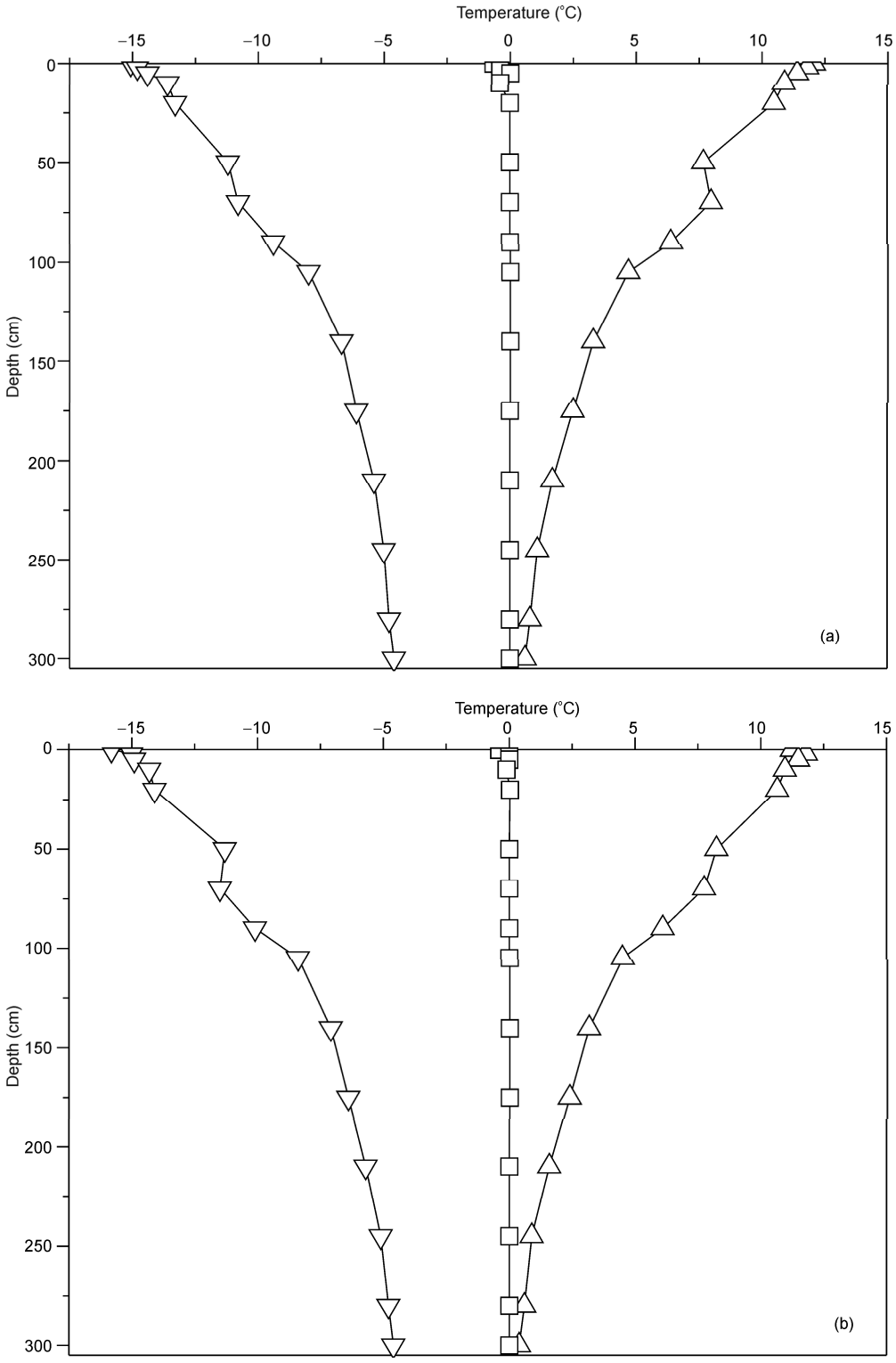

Figure 9 Measured maximum (△), minimum (▽), and freezing (□) temperatures (°C) in 2007 (a) and 2008 (b).

Based on the estimated ice content results, the energy consumed for phase change was calculated using eqs. (11) and (12). The results revealed that the release of heat was 148.73 MJ/m^2 for water-ice conversions in the freezing process of the cold season from October 2007 to March 2008 (Table 5), and the absorption of heat was 139.9 MJ/m^2 from April to September. The maximum absorption heat appeared in May, and the maximum release of heat appeared in November.

According to the assumptions from another method, the

Table 5 Monthly energy consumed for phase change (MJ/m^2) according to the modeled ice content during 2007–2008

Month	Heat flux	Month	Heat flux
6	18.35	12	–32.3
7	21.68	1	–33.8
8	23.52	2	–24.2
9	24.18	3	–7.66
10	–14.45	4	20.24
11	–36.32	5	31.93

initial water content represented the unfrozen water content when the ground surface temperature was stable and less than 0°C, i.e., the ground surface formed a stable frozen layer (Figure 9, square symbol curve). The termination water content was the minimum unfrozen water content at different depths in the active layer when the soil temperature was lowest in winter (Figure 9, inverted triangle symbol curve). The difference between the initial and termination water content was the amount of water-ice phase change (Figure 10), which can be calculated using the integral curves of the water-ice phase. The energy consumed for phase change was calculated according to the measured soil temperature and moisture in 2007 and 2008. Amounts of 0.44 m^3/m^2 (the amount of water with a cubic meter in the per square meter of soil) and 0.43 m^3/m^2 accounted for water-ice conversion in the freezing process of the cold season, and the releases of heat were 146.78 MJ/m^2 and 143.87 MJ/m^2 in 2007 and 2008 (Table 6), respectively. The average release of heat was 145.33 MJ/m^2. Compared with the results calculated by the ice content (Table 5), the energy consumed for phase change decreased by 3.4 MJ/m^2, and the relative error was 2.3%.

3.5 Future soil frost depth dynamics

The model simulates the freezing time and freezing depth (Figure 11(a)) and shows that the soil melt state was simulated in agreement with the measured values. The melt began starting from early May, and the melt depth gradually increased with increasing temperature and reached a maximum for a period of time in this state in October. A completely frozen state occurred from mid-November to early December, and the duration was shorter. The depth of simulated freezing was approximately 3.0 m, which approached

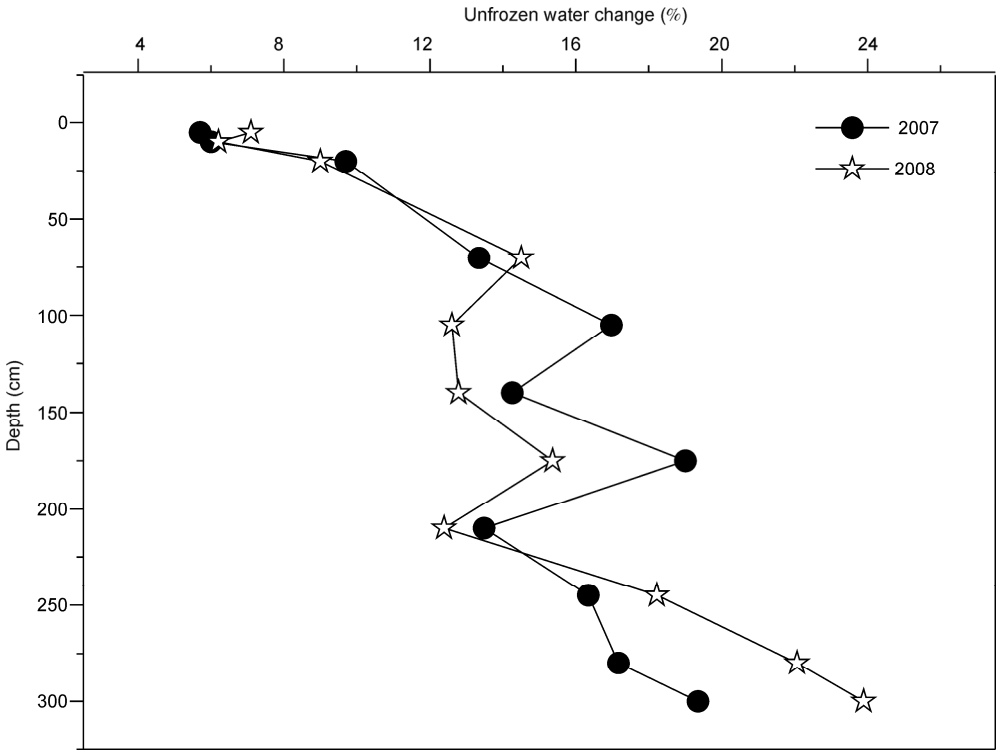

Figure 10 Measured unfrozen water content changes at different depths in 2007 and 2008.

Table 6 Energy consumed for phase change according to the measured value of the active layer of the freezing and thawing process

Year	Depth (cm)	Water-ice phase variable (m^3/m^2)	Water-ice phase change heat (MJ/m^2)
2007	300	0.44	146.78
2008	300	0.43	143.87

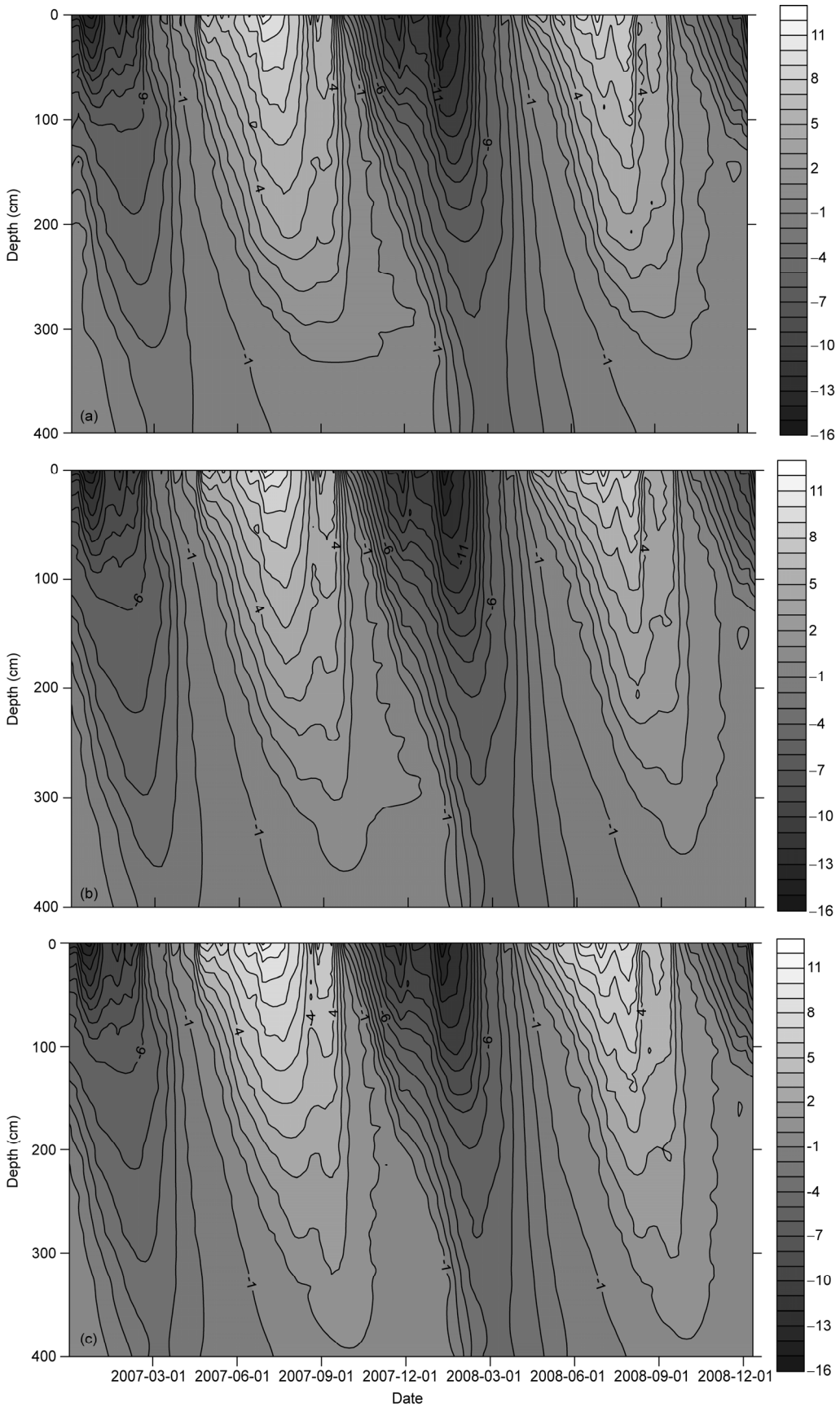

Figure 11 Simulated soil temperature for 2007–2008 (a) and simulated soil temperature for climate change scenario1: increasing air temperature by 1°C (b) and scenario2: increasing air temperature by 2°C.

the observed data value from 2007 and 2008.

Based on the calibrated model, the future soil frost depth was modeled under five scenarios. The results are shown in Figure 11(b)–(c) and reveal that the maximum active layer thickness at the Tanggula station might increase by approximately 30 and 60 cm compared with the current 330-cm active layer thickness, depending on whether the air temperature increases by 1 and 2°C, respectively. The release heat and absorption heat increased by 2.4% and 7.2% and 5.3% and 8.3% depending on whether the air temperature increases by 1 or 2°C, respectively. The sensitivity of the active layer thickness with respect to precipitation was assessed by applying 0 mm of precipitation (no rainfall) and 20% and 50% additional precipitation compared with the current precipitation. The results are shown in Figure 12(a)–(c) and reveal that the maximum active layer thickness is consistent with 330 cm for three precipitation change scenarios (Table 7). Energy consumed for phase change decreased with no precipitation and increased with 20% and 50% additional precipitation in 2007 and 2008 (Table 6). The release heat and absorption heat decreased by 5.6% and 7.5% and increased by 1.2% and 3.3% and 4.5% and 7.0% with 20% and 50% more precipitation. The results reveal that the soil moisture increased when precipitation increased due to the increase in the release of heat in the process of water-ice conversion.

4 Discussions

In this study, the simulation depth in the soil was extended to approximately 17 m, and the calibrated model satisfactorily simulated the hydro-thermal characteristics and surface heat at the Tanggula test site. There is large difference at depth of about 1 m below surface during summer months, one reason is that the thermal conduction decreases with increasing water content of the upper soil layer during the soil thawing period (Zhou et al., 2013). Another is the inaccuracy of the soil parameters. Yang et al. (2010) showed that the simulated soil temperature and moisture agreed well with the CoupModel values for the Heihe Mountains in Northwest China. This model also successfully simulated the freeze-thaw processes within the active layer (Hu et al., 2013). These studies assumed a zero heat-flux lower boundary condition, and the simulation depth with COUPMODEL was only 200 cm (Yang et al., 2010; Hu et al., 2013). This depth is not adequate to meet the observational temperature amplitudes at a mean depth of approximately 15 m over the hinterland of QXP. After the extension of the model depth and calibration, the soil temperatures at all of the layers were simulated (including the shallow, middle and deeper layers and moisture), although some discrepancies were observed between the simulated unfrozen water content and the field observations (Figures 2–4). This result could be explained by that the surface soil temperature and moisture were influenced by the weather conditions. Overall, the results accurately reflect the field observations and indicate that the model is able to reveal the hydro-thermal characteristics and is applicable in permafrost regions of the Qinghai-Xizang (Tibet) Plateau of China.

The partitioning fluxes of net radiation (H, LE, and G) were simulated for two years. The net radiation (R_n) during the 2-year study period was less than the measure value, most likely because of errors in the initial snow depth. Additionally, the net radiation was greater than the measured value from November 2008 (Figure 6(a)–(d)). In fact, the snowfall was much greater, and the daily average was between 11−21 mm from late October 2008 (data from the 20 October to 21 December). The seasonal variability in the monthly LE differed over the two years, partially because of the different seasonal patterns of precipitation. Because of the evaporation from the soil that occurred in summer, nearly all the smallest negative values of the monthly sensible heat flux (H) were obtained in response to the values of monthly LE. However, the results closely followed the pattern of the observed net radiation. The soil heat flux at depths of 0–20 cm was well simulated. The simulation accuracy was improved, which may be related to the depth from the natural ground surface and how the surface soil heat flux was calculated (Figure 5) together with the depth. The average of the annual G was approximately 0 W/m^2 (Figure 7), demonstrating that the major interest is in the partitioning into latent heat and sensible heat fluxes during the year (Wu et al., 2011a).

The energy consumed for phase change results from Zhao (2004) showed an annual value of 110 MJ/m^2 in the different vegetation zones of the permafrost regions in the QXP (Table 8). Using the same method, the releases of heat were 146.78 and 143.87 MJ/m^2 in 2007 and 2008, respectively, at the Tanggula test site. The results calculated from the estimated ice content were 148.73 and 139.9 MJ/m^2, which were closed to the results of the previous method. In contrast to this method, the energy consumed for phase change was calculated from the ice content with the actual match and showed the typical seasonal patterns. However, the vegetation type of TGL was the same as Wuli, but the results were greater than 112 MJ/m^2 due to the deeper active layer thickness. The Tanggula station was more than 3.0 m larger than the Wuli on the QXP, and the energy consumed for phase change was close to that of the Liangdao River because the vegetation type was a bog meadow, and the water content was higher with an active layer thickness of only 110 cm. It can be observed that the energy consumed for phase change was related to the soil moisture (Zhao, 2004), active layer thickness, and vegetation type and fully reflected the process of freezing and thawing of the active layer to reduce the annual changes in the amplitude of the ground temperature.

The depth of simulated freezing was greater than 3.0 m, which approached the value from the observed data in 2007

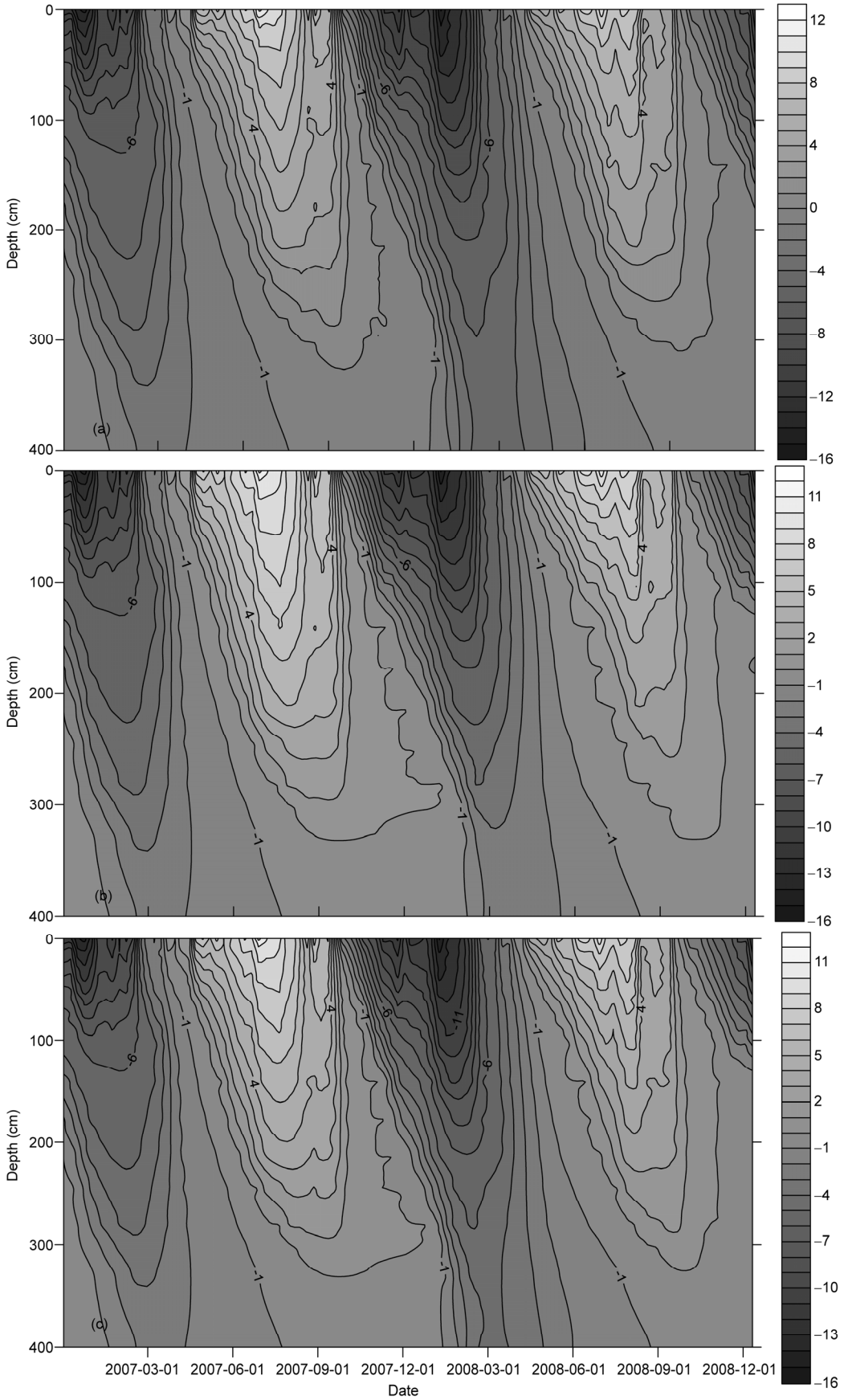

Figure 12 Simulated soil temperature for climate change scenario 3: (a) no precipitation, (b) with 20% more precipitation, (c) with 50% more precipitation.

Table 7 Simulated cumulative ground heat and energy consumed for phase change flux for different climate change scenarios

Climatic factors		Air temperature			Precipitation		
Scenarios		Current	T_{air}+1	T_{air}+2	No Prcp	Prcp+20%	Prcp+50%
Energy consumed for phase change	Release	148.73	152.27	159.43	140.42	150.56	155.38
	Absorption	139.9	147.32	151.54	137.59	144.47	149.65

Table 8 The energy consumed for phase change of active layer during the freezing and thawing process (Zhao, 2004)

Site	Vegetation types	Active layer thickness (cm)	Water-ice phase variable (m^3/m^2)	
Fenghuo mountain	Alpine meadow	137	0.34	114
Ecological station	Degraded steppe	165	0.35	118
Wuli station	Alpine steppe	260	0.33	112
Liangdao River	Bog meadow	110	0.40	135

and 2008. This result showed that the simulation of the model for the freezing depth was consistent with the measured value (Li et al., 2012). This study reveals that the maximum active layer thickness at the Tanggula station may increase by approximately 30 and 60 cm compared with the current 330 cm active layer thickness, depending on whether an air temperature increase of 1 or 2°C was used, respectively. Zhou et al. (2013) found that the maximum thaw depth in the summer may increase from approximately 20 or 50 cm compared with the current 150-cm active layer thickness with an air temperature increase of 1 or 2°C. The observed evidence shows that the permafrost in the QXP has been warming, thawing, and degrading over the past few decades, and the mean annual air temperatures from four National Weather Service Stations show an increase of approximately 0.6 to 1.6°C from 1996 to 2006 (Cheng and Wu, 2007; Wu and Zhang, 2008), and the active thickness has deepened by 10–40 cm from 1995 to 2004 in the permafrost regions (Wu and Liu, 2004; Wu et al., 2006; Yang et al., 2004). These results were quite similar to the model results. From another point of view, the distribution height of the permafrost bottom in 1990 over the Plateau ascended by approximately 71 m compared with the value from 1960 (Wang et al., 2002). Under the 0.02°C/a air-temperature rise (IPCC low value), the permafrost area in the QXP will shrink by approximately 8.8% in the next 50 years, and high temperature permafrost with a mean annual ground temperature (MAGT) greater than –0.11°C may turn into seasonal frozen soils (Nan et al., 2005). All results indicated that permafrost will be degraded with climate warming, but the degradation rates varied in different situations and different regions (Zhao et al., 2004, 2010).

The effect of additional precipitation on the soil active layer thickness was rather limited. In this paper, the maximum active layer thickness was consistent with 330 cm for three precipitation change scenarios. Compared with the influence on the air temperature changes, the precipitation change effect on the permafrost was not significant (Xiao, 2013) which is considered mainly a result of the relatively coarse soil particle with a limited water holding capacity. Hollesen et al. (2011) predicted the active layer thickness under future scenarios, and the results revealed that no further effect on the active layer thickness was observed with 20% and 50% additional precipitation. The estimated energy consumed for phase change all increased. The energy consumed for phase change decreases with no precipitation and increases with 20% and 50% additional precipitation in 2007 and 2008, respectively. This result revealed that the soil moisture becomes larger when precipitation increases due to the increased release of heat in the process of water-ice conversion, the latent heat flux was significantly increased in the precipitation days in the winter and spring (Sun et al., 2014). The model reflected the interaction between the air temperature and precipitation, and the results all demonstrated that climate warming is expected cause the permafrost active layer to deepen and change, consistent with the observed evidence. These results indicate more attention should be focused on permafrost degradation in the QXP, which could have significant impacts on hydrological conditions (Niu et al., 2011), biogeochemical processes (Nelson, 2003; Smith et al., 2005), vegetation change (Sturm et al., 2005), and carbon balance (Koven et al., 2011) and might further exert positive feedback on the climate system. Meanwhile, the soil water flow changed in frozen soil or partly frozen soils should dig deeper in the future.

5 Conclusions

This study applied the COUPMODEL for modeling of fully coupled heat transport and water flow for permafrost regions. The model results demonstrated that COUPMODEL is able to describe the hydro-thermal processes and surface energy balance in the QXP. The ice content was well estimated and the phase heat was accurately calculated using this model. Use of the model for predicting changes in the

active layer in response to 1 and 2°C of warming indicates that the maximum active layer thickness may increase from the current measure of 330 cm to approximately 358 cm and 389 cm as a result of the 1 and 2°C warming, respectively, as well as increases in the energy consumed for phase change in the processes of release and absorption. Under the different precipitation scenarios, the modeling results indicate that the energy consumed for phase change could increase as a result of 20% and 50% greater precipitation, but the estimated the energy consumed for phase change decreased with no precipitation. However, the model was only applied to a single point in this study. Further studies should address such issues as the simulated surface heat fluxes, which represent an important output of the model. Furthermore, it would be of interest to compare these values with the fluxes produced by regional climate models (Wu et al., 2011) and different underlying surfaces. It also would be of value to test the ability of COUPMODEL to simulate similar conditions for more complex systems that include dynamic vegetation and soil surface snow cover.

This work was financially supported by the National Major Scientific Project of China (Grant No. 2013CBA01803), the National Natural Science Foundation of China (Grant Nos. 41271081, 41271086), and the Foundation of One Hundred Person Project of the Chinese Academy of Sciences (Grant No. 51Y551831). We acknowledge the West Light Foundation of the Chinese Academy of Sciences. The authors also gratefully acknowledge Professor Lars Lövdahl for his constructive comments.

Alexeev V A, Nicolsky D J, Romanovsky V E, Lawrence D M. 2007. An evaluation of deep soil configurations in the CLM3 for improved representation of permafrost. Geophys Res Lett, 34: L090502

Allison I, Barry R G, Goodison B E. 2001. Climate and Cryosphere (CLIC) Project Science and Co-ordination Plan (Version 1), WCRP-114, WMO/TD No.1053, 1–96

Brown J, Romanovsky V, Vladimir E. 2008. Report from the International permafrost association: State of permafrost in the first decade of the 21st Century. Permafrost Periglacial Process, 19: 255–260

Buteau S, Fortier R, Delisle G, Allard M. 2004. Numerical simulations of the impacts of climate warming on a permafrost mound. Permafrost Periglacial Process, 15: 41–57

Cheng G D, Wu T H. 2007. Responses of permafrost to climate change and their environmental significance, Qinghai-Tibet Plateau. J Geophys Res, 112: 1–10

Cheng G D, Zhao L. 2000. The problems associated with permafrost in the development of the Qinghai-Xizang Plateau (in Chinese). Quat Sci Rev, 20: 521–531

Cheng G D. 1990. Recent development of geocryological study in China (in Chinese). Acta Geogr Sin, 45: 220–223

Cheng Z G, Liu X D, Fan G Z, Bai A J, Wang B Z. 2011. Spatiotemporal distribution of climate change over the Qinghai-Tibetan Plateau in 21st Century (in Chinese). Arid Zone Res, 28: 669–676

Demchenko P F, Eliseev A V, Arzhanov M M, Mokhov I I. 2006. Impact of global warming rate on permafrost degradation. Izv Atmos Ocean Phy, 42: 32–39

Eckersten H, Blomback K, Katterer T, Nymana P. 2001. Modelling C, N, water and heat dynamics in winter wheat under climate change in southern Sweden. Agric Ecosyst Environ, 86: 221–235

Franchini M, Pacciani M. 1991. Comparative analysis of several conceptual rainfall-runoff models. J Hydrol, 122: 161–219

Gao Z Q, Chae N, Kim J, Hong J, Choi T, Lee H. 2004. Modeling of surface energy partitioning, surface temperature and soil wetness in the Tibetan prairie using the simple biosphere model 2(SiB_2). J Geophys Res, 102: D06102

Guglielmin M, Dramis F. 1999. Permafrost as a climatic indicator in northern Victoria Land, Antarctica. Ann Glaciol, 29: 131–135

Hansson K, Simunek J, Mizoguchi M, Lundina L, Van Genuchten M. 2004. Water flow and heat transport in frozen soil: Numerical solution and freeze-thaw applications. Vadose Zone J, 3: 693–704

Harlan R L. 1973. Analysis of coupled heat-fluid transport in partially frozen soil. Water Resour Res, 9: 1314–1323

Henry K, Smith M. 2001. A model-based map of ground temperatures for the permafrost regions of Canada. Permafrost Periglacial Process, 12: 389–398

Hinkel K M, Nelson F E. 2003. Spatial and temporal patterns of active layer thickness at circumpolar active layer monitoring (CALM) sites in northern Alaska, 1995–2000. J Geophys Res, 108: 8168

Hollesen J, Elberling B, Jansson P E. 2011. Future active layer dynamics and carbon dioxide production from thawing permafrost layers in Northeast Greenland. Glob Change Biol, 17: 911–926

Hu G J, Zhao L, Li R, Wu T H, Xiao Y, Jiao K Q, Qiao Y P, Jiao Y L. 2013. The Water-thermal characteristics of frozen soil under freeze-thaw based on CoupModel (in Chinese). Sci Geogr Sin, 33: 356–362

Hu H P, Ye B S, Zhou Y H, Tian F Q. 2006. A land surface model incorporated with soil freeze/thaw and its application in GAME/Tibet. Sci China Ser D-Earth Sci, 49: 1311–1322

Ikard S J, Gooseff M N, Barrett J E, Takacs-Vesbach C. 2009. Thermal characterization of active layer across a soil moisture gradient in the McMurdo dry valleys, Antarctica. Permafrost Periglacial Process, 20: 389–398

IPCC. 2007. Climate Change Synthesis Report. Cambridge: Cambridge University Press

Jansson P E, Karlberg L. 2004. Theory and practice of coupled heat and mass transfer model for soil-plant-atmosphere system (in Chinese). In: Zhang H J, Cheng J H, Wang W. Translation. Beijing: Science Press

Jansson P E, Moon D. 2001. A coupled model of water, heat and mass transfer using object orientation to improve flexibility and functionality. Environ Modell Softw, 16: 37–46

Jiang Y Y, Zhuang Q L, O'Donnell. 2012. Modeling thermal dynamics of active layer soils and near-surface permafrost using a fully coupled water and heat transport model. J Geophys Res, 117: D11110

Jiang Z H, Zhang X, Wang J. 2008. Projection of climate change in China in the 21st century by IPCC-AR4 Models. Geogr Res, 27: 787–799

Kane D L, Hinzman L D, Zarling J P. 1991. Thermal response of the active layer to climate warming in a permafrost environment. Cold Reg Sci Technol, 19: 111–122

Koven C D, Ringeval B, Friedlingstein P, Ciaisa P, Cadulea P, Khvorostyanovd D, Krinnere G, Tarnocaif C. 2011. Permafrost carbon-climate feedbacks accelerate global warming. Proc Natl Acad Sci USA, 108: 14769–14774

Li R, Zhao L, Ding Y J, Wu T H, Xiao Y, Du E J, Liu G Y, Qiao Y P. 2012. Temporal and spatial variations of the active layer along the Qinghai-Tibet Highway in a permafrost region. Chin Sci Bull, 57: 2867–2871

Liu X D, Chen B D. 2000. Climatic warming in the Tibetan Plateau during recent decades. Int J Climatol, 20: 1729–1742

Lunardini V J. 1996. Climatic warming and the degradation of warm permafrost. Permafrost Periglacial Process, 7: 311–320

Luo D L, Jin H J, Marchenko S, Romanovsky V. 2014. Distribution and changes of active layer thickness (ALT) and soil temperature (TTOP) in the source area of the Yellow River using the GIPL model. Sci China Earth Sci, 57: 1834–1845

Luo S Q, Lü S H, Zhang Y, Hu Z Y, Ma Y M, Li S S, Shang Y L. 2008. Simulation analysis on land surface process of BJ site of central Tibetan Plateau using CoLM (in Chinese). Plateau Meteorol, 27: 259–271

Ma Z G, Wei H L, Fu C B. 1999. Progress in the research on the relationship between soil moisture and climate change (in Chinese). Adv Earth Sci, 14: 299–305

McGechan M B, Graham R, Vinten A J A, Douglasc J T, Hoodad P S. 1997. Parameter selection and testing the soil water model SOIL. J Hydrol, 195: 312–334

Nan Z T, Li S X, Cheng G D. 2005. Prediction of permafrost distribution on the Qinghai-Tibet Plateau in the next 50 and 100 years. Sci China Ser D-Earth Sci, 48: 797–804
Nassar I N, Horton R, Flerchinger G N. 2000. Simultaneous heat and mass transfer in soil columns exposed to freezing/thawing conditions. Soil Sci, 165: 208–216
Nelson F E. 2003. (Un) frozen in time. Science, 299: 1673–1675
Nicolsky D J, Romanovsky V E, Alexeev V A, Lawrence D M. 2007. Improved modeling of permafrost dynamics in a GCM land-surface scheme. Geophys Res Lett, 34: L080501
Niu L, Ye B S, Li J, Sheng Y. 2011. Effect of permafrost degradation on hydrological processes in typical basins with various permafrost coverage in Western China. Sci China Earth Sci, 4: 615–624
Oelke C, Zhang T J. 2004. A model study of circum-arctic soil temperature. Permafrost Periglacial Process, 15: 103–121
Pavlov A V. 1994. Current change of climate and permafrost in the Arctic and sub-Arctic of Russia. Permafrost Periglacial Process, 5: 101–110
Poutou E, Krinner G, Genthon C, de Noblet-Ducoudré N. 2004. Role of soil freezing in future boreal climate change. Clim Dynam, 23: 621–639
Riseborough D W, Shiklomanov N I, Etzelmuller B, Gruber S, Marchenko S. 2008. Recent advances in permafrost modeling. Permafrost Periglacial Process, 19: 137–156
Riseborough D W. 2002. The mean annual temperature at the top of permafrost, the TTOP model, and the effect of unfrozen water. Permafrost Periglacial Process, 13: 137–143
Scherler M, Hauck C, Hoelzle M, Stähli M, Völksch I. 2010. Meltwater Infiltration into the Frozen Active Layer at an Alpine Permafrost Site. Permafrost Periglacial Process, 21: 325–334
Shoop S A, Bigl S R. 1997. Moisture migration during freeze and thaw of unsaturated soils: Modeling and large scale experiments. Cold Reg Sci Technol, 25: 33–45
Smith L C, Sheng Y, MacDonald G M, Hinzman L D. 2005. Disappearing arctic lakes. Science, 308: 1429
Smith M W, Riseborough D W. 2002. Climate and the limits of permafrost: A zonal analysis. Permafrost Periglacial Process, 13: 1–15
Sridhar V, Elliott R L, Chen F, Brotzge J A. 2002. Validation of the NOAH-OSU land surface model using surface flux measurements in Oklahoma. J Geophys Res, 107(D20): ACL 3-1-ACL 3-18
Stendel M, Christensen J H. 2002. Impact of global warming on permafrost conditions in a coupled GCM. Geophys Res Lett, 29: 1632
Sturm M, Douglas T, Racine C, Liston G E. 2005. Changing snow and shrub conditions affect albedo with global implications. J Geophys Res, 110: G01004
Sun L C, Zhao L, Li R, Yao J M, Liu Y, Qiao Y P, Jiao K Q. 2014. Effects of precipitation on the permafrost ground surface energy fluxes. J Longdong Univ, 25: 41–46
Tang M C, Shen Z B, Chen Y Y. 1979. On climatic characteristics of the Xizang Plateau monsoon (in Chinese). Acta Geogr Sin, 34: 33–42
Tian H, Wei C, Wei H, Zhou J Z. 2014. Freezing and thawing characteristics of frozen soils: Bound water content and hysteresis phenomenon. Cold Reg Sci Technol, 103: 74–81
Vinnikov K Y, Robock A, Speranskaya N A. 1996. Scales of temporal and spatial variability of mid-latitude soil moisture. J Geophys Res, 101: 7163–7174
Wang C H, Shi R. 2007. Simulation of the land surface processes in the Western Tibetan Plateau in summer (in Chinese). J Glaciol Geocryol, 29: 73–81
Wang Y B, Gao Z Y, Wen J, Liu G H, Geng D, Li X B. 2014. Effect of a thermokarst lake on soil physical properties and infiltration processes in the permafrost region of the Qinghai-Tibet Plateau, China. Sci China Earth Sci, 57: 2357–2365
Wang Q C, Li L, Li D L, Qin N S, Wang Z Y, Zhu X D, Shi X H. 2005. Response of permafrost over Qinghai Plateau to climate warming (in Chinese). Plateau Meteorol, 24: 708–713
Wei Z, Jin H J, Zhang J M, Yu S P, Han X J, Ji Y J, He R X, Chang X L. 2011. Prediction of permafrost changes in Northeastern China under a changing climate. Sci China Earth Sci, 6: 924–935
Wu Q, Zhang T J. 2008. Recent permafrost warming on the Qinghai-Tibetan Plateau. J Geophys Res, 113: 1–22
Wu Q B, Cheng G D, Ma W, Niu F, Sun Z Z. 2006. Technical approaches on permafrost thermal stability for Qinghai-Tibet Railway. Geomech Geoeng, 1: 119–127
Wu Q B, Liu Y Z. 2004. Ground temperature monitoring and its recent change in Qinghai-Tibet Plateau. Cold reg Sci Technol, 38: 85–92
Wu Q B, Shen Y P, Shi B. 2003. Relationship between frozen soil together with its water-heat process and ecological environment in the Tibetan Plateau (in Chinese). J Glaciol Geocryol, 25: 250–255
Wu S H, Jansson P E, Zhang X Y. 2011. Modeling temperature, moisture and surface heat balance in bare soil under seasonal frost conditions in China. Eur J Soil Sci, 62: 780–796
Wu S H, Jansson P E, Kolari P. 2012. The role of air and soil temperature in the seasonality of photosynthesis and transpiration in a boreal scots pine ecosystem. Agr Forest Meteorol, 156: 85–103
Wu S H, Jansson P E, Kolari P. 2011. Modeling seasonal course of carbon fluxes and evapotranspiration in response to low temperature and moisture in a boreal Scots pine ecosystem. Ecol, 222: 3103–3119
Wu J C, Sheng Y, Wu Q B, Wen Z. 2010. Processes and modes of permafrost degradation on the Qinghai-Tibet Plateau. Sci China Earth Sci, 1: 150–158
Xiao Y, Zhao L, Dai Y J, Li R, Pang Q Q, Yao J M. 2013. Representing permafrost properties in CoLM for the Qinghai-Xizang (Tibetan) Plateau. Cold Reg Sci Technol, 87: 68–77
Xiao Y, Zhao L, Li R, Yao J M. 2011. Seasonal variation characteristics of surface energy budget components in permafrost regions of Northern Tibetan Plateau (in Chinese). J Glaciol Geocryol, 33: 1033–1037
Xiao Y.2013.A Study on Water-Heat Processes and Simulation along the Qinghai-Tibet Highway in Permafrost Regions (in Chinese). Doctoral Dissertation. Chinese Academy of Sciences
Yang J P, Ding Y J, Chen R S. 2004. Permafrost change and its effect on eco-environment in the source regions of the Yangtze and Yellow Rivers (in Chinese). J Mt Sci, 22: 278–285
Yang Y, Chen R S, Ji X B, Qing W W, Liu J F, Han C T. 2010. Heat and water transfer processes on alpine meadow frozen grounds of Heihe mountainous in Northwest China (in Chinese). Adv Water Sci, 21: 30–34
Yao J M, Zhao L, Ding Y J, Gu L L, Jiao K Q, Qiao Y P, Wang Y X. 2008. The surface energy budget and evapotranspiration in the Tanggula region on the Tibetan Plateau. Cold Reg Sci Technol, 52: 326–340
Zhang S L, Lövdahl L, Grip H, Jansson P E, Tong Y. 2007. Modelling the effects of mulching and fallow cropping on water balance in the Chinese Loess Plateau. Soil Till Res, 100: 311–319
Zhang T J. 2005. Influence of the seasonal snow cover on the ground thermal regime: An overview. Rev Geophys, 43: RG4002
Zhang Y W, Lü S H, Li D L, Huang J. 2003. Numerical simulation of freezing soil process on Qinghai-Xizang Plateau in early winter (in Chinese). Plateau Meteorol, 22: 471–477
Zhao L, Li R, Ding Y J. 2008. Simulation on the soil water-thermal characteristics of the active layer in tanggula range (in Chinese). J Glaciol Permafrost Eng, 30: 930–937
Zhao L, Ping C L, Yang D Q, Cheng G D, Ding Y J, Liu S Y. 2004. Changes of climate and seasonally frozen ground over the past 30 years in Qinghai-Xizang (Tibetan) Plateau, China. Global Planet Change, 43: 19–31
Zhao L, Wu Q B, Marchenko S S, Sharkhuu N. 2010. Thermal state of permafrost and active layer in Central Asia during the International Polar Year, Permafrost Periglacial Process, 21: 198–207
Zhao L. 2004. The freezing-thawing processes of active layer and changes of seasonally frozen ground on the Tibetan plateau (in Chinese). Doctoral Dissertation. Chinese Academy of Sciences
Zhou J, Kinzelbach W, Cheng G D, Zhang W, He X B, Ye B S. 2013. Monitoring and modelling the influence of snow pack and organic soil on a permafrost active layer, Qinghai-Tibetan Plateau of China. Cold Reg Sci Technol, 90-91: 38–52